



1 **Ecosystem-specific patterns and drivers of global reactive iron**
2 **mineral-associated organic carbon**

3 Bo Zhao¹, Amin Dou¹, Zhiwei Zhang¹, Zhenyu Chen¹, Wenbo Sun¹, Yanli Feng¹,
4 Xiaojuan Wang², Qiang Wang^{1,*}

5 ¹*State Key Laboratory of Herbage Improvement and Grassland Agro-ecosystems,*
6 *College of Pastoral Agriculture Science and Technology, Lanzhou University, Lanzhou*
7 *730000, China*

8 ²*Natural History Research Center, Shanghai Natural History Museum, Shanghai*
9 *Science & Technology Museum, 200127 Shanghai, China*

10 ***Corresponding author:** Qiang Wang (Phone: +86-136-6933-7869; Email:
11 wqiang@lzu.edu.cn)

12 **Type of paper:** Research Paper; Text pages: 24; Figures: 7



13 Abstract

14 Reactive iron (Fe) oxides are vital for long-term soil/sediment organic carbon (SOC)
15 storage. However, the patterns and drivers of Fe-associated organic carbon (Fe-OC)
16 over global geographic scales under various ecosystem types remain largely
17 controversial. Here, we provided for the first time a systematic assessment of the
18 distribution patterns and determinants of Fe-OC content and its contribution (*f*Fe-OC)
19 by assembling a global dataset comprising 862 observations from 325 sites in distinct
20 ecosystems. We found that Fe-OC content across global ecosystems ranged from 0 to
21 83.3 g/kg (*f*Fe-OC ranged from 0 to 82.4%), reflecting the high variability of the Fe-
22 OC pool. Fe-OC contents varied with ecosystem type, being greater in wetlands with a
23 high molar ratio of Fe-OC/dithionite-extractable Fe (Fe_d) compared with marine and
24 continental ecosystems. Furthermore, *f*Fe-OC in wetlands was significantly lower than
25 that in other ecosystems due to rich OC. In contrast with climate variables and soil pH,
26 the random forest modelling and multivariate analysis showed that the Fe-OC: Fe_d and
27 SOC were the predominant predictors of Fe-OC content and *f*Fe-OC in wetlands and
28 continents, whereas Fe_d content was a primary driver in marine ecosystems. Based on
29 upper estimates of global SOC storage in various ecosystem types, we further estimated
30 that 83.84 ± 3.86 Pg, 172.45 ± 8.74 Pg, and 24.48 ± 0.87 Pg of SOC were preserved by
31 association with Fe oxides in wetlands, continental and marine ecosystems, respectively.
32 Taken together, our findings highlighted the importance of reactive Fe oxides in global
33 SOC preservation, and their controlling factors were ecosystem-specific.

34 **Keywords:** Ecosystem type, mineral protection, reactive iron oxides, iron-bound



35 organic carbon, organic carbon preservation



36 **1. Introduction**

37 The global soil (sediment) organic carbon (SOC) cycle has become one of the
38 hotspots in biogeochemical and global climate change research (Lal, 2004a; Crowther
39 et al., 2016). Organic carbon (OC) sequestration is a significant ecosystem service (such
40 as climate mitigation, soil fertility and ecosystem stability, etc.) provided by terrestrial,
41 wetland, and marine ecosystems. Accumulating evidence has shown that the reactive
42 mineral matrix plays a critical role in sequestering and stabilizing SOC (Kramer and
43 Chadwick, 2018; Ye et al., 2022). OC has a strong affinity for reactive Fe (hydr-)oxides
44 (Longman et al., 2022), and the resulting Fe and OC association by adsorption or
45 coprecipitation is thought to promote OC long-term preservation in soils and sediments
46 (Schmidt et al., 2011; Hemingway et al., 2019). Therefore, a systematic understanding
47 of the patterns and drivers of Fe-associated OC (Fe-OC) is pivotal for accurately
48 predicting SOC dynamics and reducing model uncertainties in forecasting carbon-
49 climate feedback at the global scale.

50 In comparison to other metal minerals, Fe (hydr-)oxides, one of the most prevalent
51 reactive minerals, have larger specific surface areas, a higher OC affinity, and a greater
52 potential to retain SOC (Guggenberger and Kaiser, 2003; Eusterhues et al., 2005; Kaiser
53 et al., 2007). A growing body of studies has suggested that Fe (hydr-)oxides play a
54 fundamental role in stabilizing SOC in sediment and soil (Yu et al., 2021). Recently,
55 Fe-OC has been extracted and quantified through the bicarbonate-citrate-dithionite
56 (BCD) method, and was estimated to constitute 21.5% (Lalonde et al., 2012), 4.7–37.8%
57 (Zhao et al., 2016; Fang et al., 2019; Zong et al., 2021), and 3.4–11.8% (Huang et al.,



58 2021; Wang et al., 2021) of SOC in marine sediments, continents (i.e., forests,
59 grasslands, farmland) and wetlands (i.e., coastal, peatland, and lake wetlands),
60 respectively. The Fe-OC content and contribution (*f*Fe-OC) vary with ecosystem type.
61 Marine sediments are the largest OC sink on Earth and are crucial to the global carbon
62 cycle. Reactive Fe minerals can protect and bury large amounts of SOC within marine
63 sediments, constituting a “rusty sink” (Lalonde et al., 2012). The *f*Fe-OC in marine
64 sediments is significantly lower than that in offshore estuarine sediments due to
65 differences in sediment mineralogy, reactive Fe source and organic matter composition
66 (Longman et al., 2022). It is well known that wetland ecosystems possess an extremely
67 high rate of OC sequestration (McLeod et al., 2011; Hopkinson et al., 2012). Compared
68 with continental and marine ecosystems, wetland soils or sediments are periodically
69 submerged due to (semi)diurnal tidal cycles or fluctuations in the water table (Yu et al.,
70 2021). Thus, in wetland environments, Fe (hydr-)oxides are repeatedly formed and
71 destroyed as a result of periodical redox-induced changes in Fe²⁺/Fe³⁺ (Patzner et al.,
72 2020), which is thought to weaken the interaction between Fe and OC (Huang and Hall,
73 2017; LaCroix et al., 2019; Anthony and Silver, 2020). However, Wang et al. (2017)
74 proposed an important “iron gate” mechanism in OC-rich wetlands (Wang et al., 2017),
75 and showed that the contribution of Fe-OC to SOC (*f*Fe-OC) in wetlands and uplands
76 is equally important (Wang et al., 2017). Thus, a systematic analysis of Fe-OC content
77 and *f*Fe-OC in continental, wetland and marine ecosystems at the global scale can
78 provide evidence for the importance of reactive Fe minerals in global climate change.

79 Recently, some studies have found that the Fe-OC content and *f*Fe-OC are mainly



80 controlled by soil properties (Grybos et al., 2009; Ye et al., 2022), organic matter
81 composition (Fisher et al., 2020), and climate (or latitude) (Kramer and Chadwick,
82 2018). For instance, Fe-OC increases with increasing latitude, mean annual
83 precipitation (MAP), SOC content, and potential evapotranspiration (Zhao et al., 2016;
84 Kramer and Chadwick, 2018), but it decreases with increasing soil pH at the continental
85 scale (Ye et al., 2022). However, Fe-OC content and *f*Fe-OC in farmland soils are not
86 related to latitude, mean annual temperature (MAT) and MAP but are related to SOC
87 content (Wan et al., 2019). In peatlands, Huang et al. (2021) found that Fe-OC content
88 is positively correlated with the SOC content, C:N, and MAT but not with MAP at the
89 regional scale (Huang et al., 2021). However, Fe-OC in coastal wetlands was positively
90 correlated with amorphous Fe content and clay content, but negatively correlated with
91 soil pH and phenol oxidase activity (Bai et al., 2021). In marine sediments, Fe-OC
92 content may be mainly responsible for SOC content and organic matter functional
93 groups (especially carboxyl content) (Wang et al., 2019; Fisher et al., 2020).
94 Additionally, according to Kramer & Chadwick (2018), *f*Fe-OC in humid climate forest
95 regions was much higher than that in semiarid and arid regions, confirming the natural
96 linkages between *f*Fe-OC and climate (Kramer and Chadwick, 2018). Fe-OC content
97 is also influenced by the bonding mechanism of Fe and OC (Wagai and Mayer, 2007;
98 Faust et al., 2021). The bonding mechanism between Fe and OC is determined by the
99 Fe-OC/dithionite-extractable Fe (Fe_d) molar ratio (Faust et al., 2021; Wang et al., 2021),
100 with less than 1 indicating an Fe-OC bonding form of monolayer surface sorption, and
101 greater than 6 indicating a bonding mechanism dominated by coprecipitation (Wagai



102 and Mayer, 2007; Lalonde et al., 2012). Generally, the OC content of the complexes
103 obtained by coprecipitation is much higher than that of adsorption (Chen et al., 2014),
104 which may also explain the wide variations in Fe-OC and *f*Fe-OC. Thus, uncovering
105 the factors controlling Fe-OC formation/association at the global scale is a prerequisite
106 for predicting the size of the OC pool and its feedback on global climate change.
107 However, the determinants of Fe-OC associations remain unknown globally, and only
108 two studies on Fe-OC have been undertaken at continental scale, which focus on the
109 relationships of Fe-OC and soil pH (Ye et al., 2022), MAP and potential
110 evapotranspiration (Kramer and Chadwick, 2018). These studies overlooked the
111 influence of climate and soil properties (such as soil pH, Fe_a, Fe-OC:Fe_a, clay content)
112 in controlling Fe-OC and *f*Fe-OC in wetland and marine ecosystems. Furthermore, they
113 have not yet explored the relationship between these key factors and Fe-OC and *f*Fe-
114 OC across global ecosystem types. A deeper understanding of these limitations in
115 continental, wetland and marine ecosystems will allow us to draw clear conclusions
116 regarding global patterns and drivers of Fe-OC.

117 In this study, we provide a comprehensive analysis of the spatial variability and
118 characteristics of Fe-OC among continental, wetland and marine ecosystems and its
119 governing factors globally. Specifically, we analysed data from 862 observations from
120 46 published papers and the National Ecological Observatory Network (NEON) to
121 explore (i) the importance of Fe-OC to SOC storage in wetland and marine ecosystems
122 and its level compared with continental ecosystems, (ii) whether the distribution
123 patterns (i.e., spatial variability) of Fe-OC and the relationships between key factors



124 and Fe-OC differ among ecosystem types? (iii) The bonding mechanism of reactive Fe
125 and OC in different ecosystem types, i.e., adsorption or coprecipitation?

126 **2. Materials and methods**

127 **2.1 Study selection**

128 The ecosystem types included continents, wetlands, and marine ecosystems in this
129 study. We conducted extensive literature searches on the Web of Science
130 (<https://www.webofscience.com>) and China National Knowledge Resource Integrated
131 databases, and searched for relevant research published from 2010 to August 2022. The
132 appropriate studies were identified by the following search terms: ('reactive mineral'
133 OR 'iron') AND ('bound' OR 'associated' OR 'stabilization' OR 'interaction' OR
134 'sequestration') AND ('organic carbon')) (Fig. S1). The following criteria must be met
135 for inclusion in this study: (a) soil samples at 0-100cm depth must be collected from in
136 situ observation data of wetlands (i.e., peatland, bog, fen, deltaic, lake wetland,
137 mangrove wetland, and estuary wetland), forests (i.e., evergreen forest, and deciduous
138 forest), grasslands (i.e., temperate grasslands and alpine grasslands), farmland (i.e.,
139 paddy field and crop), and marine ecosystems (i.e., marine and river sediments); (b) the
140 contents of Fe-OC and Fe_d were measured using the BCD method in bulk soil; and (c)
141 Fe-OC, Fe-OC/Fe_d molar ratio must be provided or could be calculated from the
142 publications. In total, we compiled 862 data records from 46 published papers, along
143 with 42 additional data collected from NEON. The dataset involved 325 sites, with
144 latitudes between 25.22°S and 81.75°N and longitudes between 156.4°W and 174.4°E
145 (Fig. 1).



146 2.2 Data assembly and collection

147 Data from published articles and NEON were assembled to construct the Fe-OC
148 dataset. Site-specific data such as ecosystem type, MAP, MAT, latitude, longitude, clay,
149 soil pH, SOC, Fe-OC, Fe_d, Fe-OC/Fe_d molar ratio, and *f*Fe-OC (calculated using the
150 following equation: $f\text{Fe-OC} (\%) = \text{Fe-OC}/\text{SOC} \times 100\%$) were collected from each
151 published paper; other details are shown in Table S1. If the MAT and MAP are not
152 reported, the data for each site shall be obtained from the WordClim database
153 (<http://www.worldclim.org.d>). All original data and average data were taken from the
154 published articles' text, graphs, and tables. When data were presented graphically, the
155 numerical data were digitized and extracted with the GetData Graph Digitizer (version
156 4.4).

157 2.3 Statistical analysis

158 All data analyses were conducted using the R platform (v 4.1.2; [https://www.r-](https://www.r-project.org/)
159 [project.org/](https://www.r-project.org/)). We used the Shapiro-Wilk test to determine the homogeneity of variances
160 and the normal distribution of the data before using parametric methods. We used the
161 Kruskal–Wallis test to determine significant differences among different ecosystems.

162 Hedges' *g*, a bias-corrected standardized mean difference, was used to measure
163 effect size to account for the bias of ecosystem-scale Fe-OC associated with small
164 sample sizes (Chien & Krumins, 2022; Smale et al., 2020). Based on ecosystem types,
165 all data were divided into continental, marine and wetland ecosystems, and the data
166 were averaged separately for each ecosystem, representing 'control'. The sample sizes
167 of individual cases (i.e., a single published article) represent 'treatment'. The



168 standardized mean difference between the ‘control’ and ‘treatment’ was measured by
169 the pooled variance (Chien & Krumins, 2022). We used the package “metafor” in R (v
170 4.1.2; <https://www.r-project.org/>) to generate forest plots for every ecosystem by using
171 a random effects model (Fig. S2). We calculated the total observed change (I^2) and used
172 heterogeneity test (Q) to verify the heterogeneity of the collected data, and an I^2 value
173 higher than 75% or $p < 0.05$ indicates substantial heterogeneity (Meisner et al., 2014).
174 We performed Spearman’s correlation analyses to evaluate the relationship between
175 environmental variables (SOC, MAT, MAP, clay, soil pH, Fe-OC:Fe_d, Fe_d, and latitude)
176 and Fe-OC and *f*Fe-OC. The linear (“lm” function in R) fitting was demonstrated to
177 analyse the relationships between environmental variables and Fe-OC and *f*Fe-OC. The
178 significant correlation was considered at $p < 0.05$. To test the relative importance of
179 these drivers, a random forest analysis (RF, Breiman, 2001) was performed according
180 to the protocol described by Delgado-Baquerizo et al. (2016). For the RF analyses, the
181 climate variables (MAT, MAP), soil properties (SOC, clay, soil pH, Fe-OC:Fe_d, and
182 Fe_d), and geographical location (i.e., latitude) were involved as predictors, and the Fe-
183 OC and *f*Fe-OC changes and dynamics as the response variables. The significance of
184 the models and cross-validated R^2 values were evaluated with 500 permutations of the
185 response variables with the “A3” R package. Similarly, using the “rfPermute” package
186 for R ($p < 0.05$), the importance of each predictor on the response variables was
187 evaluated.



188 3. Results

189 3.1 Fe-associated OC and its related indicators across ecosystem types

190 Across global ecosystem types (i.e., continental, wetland and marine ecosystems),
191 Fe-OC content ($n = 862$) and $f\text{Fe-OC}$ ($n = 855$) varied significantly and ranged from 0
192 to 83.3 mg g^{-1} (mean: $5.62 \pm 0.32 \text{ mg g}^{-1}$) and $0\text{--}82.4\%$ (mean: $16.03 \pm 0.41\%$),
193 respectively (Figs. 2a, b). The contents of Fe-OC in continental, marine and wetland
194 ecosystems were $5.42 \pm 0.41 \text{ mg g}^{-1}$ ($f\text{Fe-OC}$: $17.76 \pm 0.90\%$), $2.34 \pm 0.12 \text{ mg g}^{-1}$
195 ($f\text{Fe-OC}$: $16.32 \pm 0.58\%$) and $9.97 \pm 0.91 \text{ mg g}^{-1}$ ($f\text{Fe-OC}$: $13.70 \pm 0.63\%$),
196 respectively, with significant differences among ecosystem types ($p < 0.05$; Fig. 2a),
197 but no significant difference in $f\text{Fe-OC}$ was observed ($p > 0.05$; Fig. 2b). Meanwhile,
198 Hedges' g unbiased standardized mean difference showed that small sample sizes at
199 local scale (i.e., single published articles) had obvious distinct effect sizes for
200 ecosystem-scale Fe-OC ($I^2 > 75\%$ or $p < 0.05$), especially for marine ecosystems (Fig.
201 S2). Fe_d contents ($n = 856$) ranged from 0.03 to 245 mg g^{-1} (mean: $9.43 \pm 0.53 \text{ mg g}^{-1}$;
202 Fig. 2c); that is, Fe_d varied 8167-fold, which was significantly higher in continental
203 ecosystems than in wetland and marine ecosystems ($p < 0.05$; Fig. 2c). The Fe-OC/ Fe_d
204 molar ratio ($n = 855$) ranged from $0\text{--}331.68$ (mean: 8.40 ± 0.85) at the global scale, and
205 its mean value was significantly higher in wetlands than in continents, while the
206 minimum value was found in marine systems ($p < 0.05$; Fig. 2d). SOC contents ($n =$
207 854) ranged from 0.3 to 423.74 mg g^{-1} (mean: $43.28 \pm 2.52 \text{ mg g}^{-1}$), which had similar
208 changes with the Fe-OC contents among ecosystem types ($p < 0.05$; Fig. 2e). Taken
209 together, the Fe-OC, SOC, Fe-OC/ Fe_d molar ratio, and soil pH were significantly higher



210 in wetlands, with the lowest values in marine ecosystems across global ecosystem types.

211 **3.2. Effect of environmental factors on Fe-OC and *f*Fe-OC across ecosystem types**

212 We analysed their relationships with climate variables and soil properties to better
213 understand the potential effect factors behind the observed variance in Fe-OC contents
214 and *f*Fe-OC among ecosystem types (Fig. 3). Among them, in wetland ecosystems, Fe-
215 OC content showed a negative correlation with MAT ($R = -0.42, p < 0.001$; Fig. 3a) and
216 MAP ($R = -0.26, p < 0.001$; Fig. 3b), while *f*Fe-OC was positively correlated with the
217 climate variables (MAT, MAP) (Figs. 3i, j). The Fe-OC content decreased significantly
218 with increasing soil pH in wetlands ($R = -0.24, p < 0.01$; Fig. 3c) and continents ($R = -$
219 $0.19, p < 0.05$; Fig. 3c), but *f*Fe-OC increased with increasing soil pH ($R = 0.52, p <$
220 0.001 ; Fig. 3k) in wetlands. Across the ecosystem types, Fe_d contents showed positive
221 correlations with Fe-OC ($R = 0.25, p < 0.001$; Fig. 3g) and *f*Fe-OC ($R = 0.28, p < 0.001$;
222 Fig. 3o) in marine ecosystems only. Moreover, Fe-OC increases significantly with Fe_d
223 contents ($R = 0.35, p < 0.001$; Fig. 3g) in wetlands, but *f*Fe-OC does not; however, Fe_d
224 content has no relationship with Fe-OC and *f*Fe-OC in continental ecosystems. The
225 molar ratio of Fe-OC/Fe_d was positively correlated with Fe-OC and *f*Fe-OC in three
226 ecosystem types, except for *f*Fe-OC in wetlands (Figs. 3e, m). Fe-OC contents
227 increased significantly, but *f*Fe-OC (except marine) decreased with increasing SOC
228 contents in all ecosystems (Figs. 3f, n). At continental scales, Fe-OC content ($R = 0.35,$
229 $p < 0.001$; Fig. 3d) and *f*Fe-OC ($R = 0.44, p < 0.001$; Fig. 3l) were positively related to
230 clay content. Latitudinal patterns in Fe-OC content and *f*Fe-OC were observed across
231 global ecosystem types (Figs. 3h, p). Taken together, Fe-OC contents are significantly



232 correlated with both SOC and the Fe-OC/Fe_d molar ratio, which may be important
233 predictors of Fe-OC in global ecosystems.

234 Moreover, according to RF analysis, the Fe-OC/Fe_d molar ratio and SOC and Fe_d
235 contents were found to be the most important variables for predicting the Fe-OC content
236 and *f*Fe-OC across global ecosystem types (Fig. 4). Different controlling factors on Fe-
237 OC content and *f*Fe-OC were operational among ecosystem types. At continental scales,
238 the Fe-OC/Fe_d molar ratio was a central driver of the Fe-OC content and *f*Fe-OC, and
239 the contents of SOC and Fe_d had a more significant influence than the soil pH and
240 climate variables (MAT, MAP) (Figs. 4a, b). The largest influence on Fe-OC content
241 and *f*Fe-OC in marine ecosystem was in the order of Fe_d > Fe-OC:F_d > SOC > latitude
242 (Figs. 4c, d). In wetlands, the Fe-OC/Fe_d molar ratio was the main driver of Fe-OC,
243 whereas SOC had a more significant role than Fe_d and soil pH (Fig. 5e); For *f*Fe-OC,
244 the largest influence was in the range of SOC > Fe-OC:F_d > pH > MAT > MAP > Fe_d
245 (Fig. 4f). The role of Fe_d content in controlling Fe-OC content and *f*Fe-OC was greater
246 in marine systems than in continents and wetlands. These results revealed that drivers
247 of both Fe-OC content and *f*Fe-OC were ecosystem specific. The climate predictors
248 accounted for relatively small percentages in all ecosystems. Collectively, Fe-OC:F_d,
249 SOC, and Fe_d were all selected by RF analysis as important predictors of changes in
250 Fe-OC content and *f*Fe-OC, which agreed with the results of our Spearman's
251 correlation analyses (Fig. 3).

252 3.3. The vital role of Fe-OC:Fe_d in controlling Fe/OC interactions

253 At the continental scale, the proportions of Fe-OC/Fe_d molar ratios less than 1 (<



254 1), between 1 and 6 (1–6), and higher than 6 (> 6) were 33.10%, 47.89%, and 19.01%,
255 respectively (Fig. 5). Moreover, we found that the proportions of 1–6 were larger in
256 grasslands and farmland than in forests, but the proportions of > 6 in grasslands were
257 higher. In marine ecosystems, the proportion of $\text{Fe-OC}:\text{Fe}_d < 1$ (31.0%) is lower than
258 that of 1–6 (63.75%), and the proportion of > 6 (5.31%) is the smallest. However, the
259 proportion of $\text{Fe-OC}:\text{Fe}_d > 6$ (39.44%) in wetlands was significantly higher than that in
260 other ecosystems (19.01% and 5.31%, respectively), but the proportion of < 1 (13.55%)
261 was lower.

262 Consistent with our expectation, the molar ratio was significantly positively
263 correlated with Fe-OC and SOC contents but negatively correlated with Fe_d in all
264 ecosystem types (Fig. 6). Moreover, the results showed that MAT and MAP are also
265 major negative regulators of the molar ratio dynamics at the continental scale, whereas
266 in wetlands, it is soil pH (Figs. 6a, c).

267 4. Discussion

268 4.1 Reactive Fe promotes SOC preservation at the global scale

269 In contrast to previous studies (Kramer and Chadwick, 2018; Yu et al., 2021; Ye et
270 al., 2022), our findings suggested that a comprehensive analysis of global patterns of
271 Fe-OC associations across ecosystem types, particularly in wetland and marine
272 ecosystems, can bridge the knowledge gap in understanding the importance of global
273 SOC preservation by reactive Fe. Generally, mineral-associated organic carbon is the
274 dominant SOC pool in soil systems, with a proportion of approximately 50–80% of
275 SOC (Cotrufo et al., 2019). As an important component of reactive minerals, Fe



276 (hydr-)oxides play a fundamental role in the formation and dynamics of mineral-
277 associated organic carbon (Lalonde et al., 2012). Our findings showed that the average
278 content of Fe-OC was $5.63 \pm 0.32 \text{ mg g}^{-1}$ soil ($n = 862$), and the proportion ($f\text{Fe-OC}$)
279 of Fe-OC in total SOC was $16.03 \pm 0.41\%$ ($n = 855$) across global ecosystems (Figs.
280 2a, b), indicating that Fe-OC is essential to the persistence of SOC. Consistent with
281 our expectation, significant difference in $f\text{Fe-OC}$ was observed among different
282 ecosystem types. At the continental scale, the mean $f\text{Fe-OC}$ was $17.75 \pm 0.90\%$ (0–
283 82.36%, $n = 284$), which was consistent with findings from Tibetan alpine meadows
284 ($15.8 \pm 12.0\%$) (Fang et al., 2019) but was lower than those for continental-scale
285 forests, such as moist forests (25.3–49.8%) and wet forests (47.1–64.1%) (Zhao et al.,
286 2016; Kramer and Chadwick, 2018). According to upper estimates of global continent
287 SOC storage (971 Pg) (including forest (383 Pg), grassland (423Pg) and farmland (165
288 Pg)) (Carter et al., 2000; Lal, 2004b; Pan et al., 2011; Prentice et al., 2001), we
289 estimated that $172.45 \pm 8.74 \text{ Pg}$ of SOC was bound to Fe oxides in continental
290 ecosystems. Meanwhile, we predicted that $49.02 \pm 5.24 \text{ Pg}$ ($12.80 \pm 1.37\%$), $74.28 \pm$
291 4.95 Pg ($17.56 \pm 1.17\%$), and $28.41 \pm 4.34 \text{ Pg}$ ($17.22 \pm 2.63\%$) of SOC were associated
292 with Fe oxides in forests, grasslands, and farmlands, respectively. In contrast to
293 continental ecosystems, evidence of interactions between Fe and SOC in marine
294 sediments has been reported more often (Berner, 1970), but the potentially importance
295 of reactive Fe for SOC preservation has only recently been recognized in marine
296 sediments (Lalonde et al., 2012). Recently, an accumulating body of studies have
297 shown that reactive Fe has a strong affinity for SOC, forming stable Fe-OC complexes



298 that can persist for thousands of years in marine sediments, serving as a “rusty sink”
299 for marine sedimentary carbon (Lalonde et al., 2012; Faust et al., 2021). Our findings
300 suggested that $f\text{Fe-OC}$ in global marine sediments ranged widely from 0.51% to
301 60.3%, with a mean of $16.32 \pm 0.58\%$. These values are consistent with published
302 estimates for the East China Sea ($13.2 \pm 8.9\%$) (Ma et al., 2018), Bohai Sea ($11.5 \pm$
303 8.3%) (Wang et al., 2019), River Delta ($8.1\text{--}20.2\%$) (Shields et al., 2016), Barents Sea
304 ($10\text{--}20\%$) (Faust et al., 2021), and global marine surface sediments ($21.8 \pm 8.6\%$)
305 (Lalonde et al., 2012). Based on model-predicted global marine sedimentary OC
306 stocks (150 Pg) (Hedges & Keil, 1995), we further estimated that 24.48 ± 0.87 Pg of
307 the marine sedimentary OC was directly associated with Fe oxides, which was
308 comparable to the results of previous study (19–45 Pg OC) (Lalonde et al., 2012).
309 Wetland ecosystems, however, frequently experience seawater flooding, atmosphere
310 exposure, and/or disruption of the hydrological balance due to (semi)diurnal tidal
311 cycles or water table drawdown, in contrast to continental and marine systems (Huang
312 and Hall, 2017; Patzner et al., 2020). Fe-OC associations are weakened with the
313 reductive breakdown of Fe(III) (hydr)oxides driven by periodic soil redox processes
314 (Patzner et al., 2020). Although wetlands store 20–30% of the Earth’s soil carbon
315 (~ 2500 Pg) (Roulet, 2000; Bridgham et al., 2006), the importance of Fe-OC in wetland
316 soils/sediments remains controversial. In global wetlands, we found that the absolute
317 content of Fe-OC was significantly higher than those in continental and marine
318 ecosystems, whereas the opposite was true for $f\text{Fe-OC}$, which was significantly lower
319 in wetlands. Our findings in wetlands were also consistent with those of Ye et al. (2022)



320 at continental scales ($13.6 \pm 1.0\%$; Ye et al., 2022) and regional-scale wetlands (16.1
321 $\pm 1.4\%$) (Wang et al., 2021) but were higher than those for specific peatland
322 ecosystems ($3.42 \pm 1.32\%$) (Huang et al., 2021). Compared with coastal wetlands (for
323 instance, mangrove wetland and tidal wetland) (Bai et al., 2021; Zhao et al., 2022),
324 inland wetlands (for instance, alpine wetland and peatland) have lower $f\text{Fe-OC}$ (Wang
325 et al., 2017; Huang et al., 2021), which may lead to significantly lower $f\text{Fe-OC}$ in
326 global wetlands. Therefore, the significance of reactive Fe minerals for SOC
327 sequestration in global wetlands may be underestimated based on peatland $f\text{Fe-OC}$
328 (Huang et al., 2022). Here, based on global wetland $f\text{Fe-OC}$ and total SOC stocks (612
329 Pg) (Yu et al., 2010), we predicted that 83.84 ± 3.86 Pg of SOC was preserved by
330 binding to Fe oxides. Collectively, these findings confirmed the fundamental role of
331 reactive Fe minerals for OC sequestration and conservation in global ecosystems.

332 Two possible mechanisms may explain the higher Fe-OC content in wetlands than
333 in other ecosystems. First, the molar ratios of $\text{Fe-OC}:\text{Fe}_d$ were significantly higher in
334 wetlands than in continental and marine ecosystems ($p < 0.05$; Fig. 2d), suggesting that
335 in wetlands reactive Fe is more effective in OC binding (Wagai and Mayer, 2007; Riedel
336 et al., 2013). Numerous studies have shown that the $\text{Fe-OC}:\text{Fe}_d$ acts as an indicator of
337 Fe/OC interaction types (Lalonde et al., 2012; Wang et al., 2017), with <1 suggesting
338 that the OC-Fe bonding form is dominated by simple mono-layer adsorption, while
339 higher ratios indicating coprecipitation (Wagai and Mayer, 2007; Faust et al., 2021).
340 Thus, compared with other ecosystems, in wetlands coprecipitation played a more
341 significant role in the binding/association of Fe-OC. Second, the SOC content in



342 wetlands was significantly higher than that in continental and marine ecosystems ($p <$
343 0.05; Fig. 2e), and it is generally believed that the SOC in wetlands has various
344 chemical bonds or chemical compositions (Wang et al., 2017; Coward et al., 2018).
345 Thus, the high SOC content in wetlands could be responsible for the predominance of
346 Fe(II) with a strong OC-complexation capacity (Jones et al., 2015; Bhattacharyya et al.,
347 2018), especially the enrichment of phenolic (Freeman et al., 2001), ultimately
348 promoting the Fe-OC association (Riedel et al., 2013; Coward et al., 2018).

349 **4.2 Ecosystem-specific relationships of Fe-OC associations with key factors**

350 The role of soil pH, SOC, Fe_d , Fe-OC: Fe_d , MAT and MAP in controlling Fe-OC
351 contents and $fFe-OC$ among ecosystem types was thoroughly analysed. A compilation
352 of global datasets including continental, wetland, and marine ecosystems demonstrated
353 that Fe-OC content and $fFe-OC$ are strongly coupled to both the Fe-OC: Fe_d molar ratio
354 and SOC content ($p < 0.001$; Figs. 3e, f, m, n), indicating that the two variables are
355 important determinants of Fe-OC content and $fFe-OC$. The results from the RF models
356 also revealed that Fe-OC: Fe_d molar ratio, SOC content, and Fe_d content were important
357 predictors of Fe-OC and $fFe-OC$ across ecosystem types (Fig. 4). Collectively, these
358 findings suggested a generic dependency of Fe-OC and $fFe-OC$ on the Fe-OC: Fe_d
359 molar ratio and SOC, regardless of their ecosystem types. Former studies on the
360 response of Fe-OC to climate variables and soil properties only concentrated on the
361 continental scale and specific ecosystems with limited data (Ye et al., 2022), making it
362 challenging to reach definitive conclusions. Kramer & Chadwick (2018) concluded that
363 continental-scale Fe-OC variation depended on MAP and potential evapotranspiration



364 but overlooked the role of soil properties (Kramer and Chadwick, 2018). Our findings
365 further showed that the soils with higher MAP were linked with lower soil pH (Fig. 6),
366 which had a positive effect on Fe-OC contents at the continental scale (Fig. 3c), and
367 these results are in line with Ye et al. (2022) (Ye et al., 2022). Furthermore, we found
368 that Fe-OC content was primarily controlled by the Fe-OC:Fe_d molar ratio at the
369 continental scale and wetlands (Fig. 7). Given the strong affinity of OC with [Fe(III)]
370 (hydr-)oxides, we speculated that an increase in Fe_d content would lead to higher Fe-
371 OC content, assuming sufficient SOC was present (Ma et al., 2018; Wang et al., 2019).
372 Although reactive Fe plays a fundamental role in OC binding, its content is not related
373 to Fe-OC content in specific terrestrial ecosystems, such as the Qinghai-Tibet Plateau
374 and regional-scale forests (Mu et al., 2016; Zhao et al., 2016). Our study, for the first
375 time, illustrated the crucial role of Fe_d in controlling Fe-OC contents and *f*Fe-OC in
376 global marine ecosystems (Fig. 3g and Fig. 4c). Previous findings indicated that
377 increased terrigenous reactive Fe inputs contributed to higher Fe-OC contents (Ma et
378 al., 2018; Wang et al., 2019). Therefore, sedimentary Fe_d content was the controlling
379 factor of Fe-OC associations in marine ecosystems. The findings of Faust et al. (2021),
380 however, who showed that a higher Fe_d content does not always enhance Fe-OC
381 associations in Arctic marine sediments, were in contrast to our findings (Faust et al.,
382 2021). The differences between our results and those of Arctic marine sediments may
383 be mainly related to the study scale. Nevertheless, the bonding mechanism of Fe and
384 OC (adsorption vs. coprecipitation) is a predominant driver of *f*Fe-OC in wetlands and
385 continental ecosystems, as illustrated by the RF analysis and a good linear correlation.



386 Given that the Fe and OC interactions are substantially controlled by Fe redox processes
387 (Riedel et al., 2013; Adhikari et al., 2016), we posited that the contents and proportions
388 of Fe-OC are governed mainly by Fe redox cycling and associated bonding mechanisms,
389 with the exception of the marine ecosystems. The results of this study suggested that
390 future climate warming may increase the proportions of Fe-OC in the total SOC,
391 especially in wetlands (Figs. 3i, j), even though additional research is necessary to fully
392 understand the effects of climate changes on Fe-OC at the global scale.

393 **4.3 Potential bonding mechanism between Fe and OC across ecosystem types**

394 Adsorption and coprecipitation are well-known to be important and well-
395 documented processes for the association of OC and reactive Fe (Lalonde et al., 2012;
396 Chen et al., 2014). Reactive Fe can act as sorbents of OC to adsorb large amounts of
397 OC to mineral surfaces due to its ubiquity in the environment, high surface area and
398 small particle size (Kaiser and Guggenberger, 2003). Riedel et al. (2013) showed that
399 coprecipitated Fe-OC complexes form when reduced Fe is oxidized in the presence of
400 dissolved OC at the oxic-anoxic interface and present a high Fe-OC:Fe_d molar ratio
401 (Riedel et al., 2013). The Fe-OC:Fe_d molar ratio can be used as an indicator for the
402 bonding mechanism between Fe and OC (Lalonde et al., 2012; Peter and Sobek, 2018;
403 Faust et al., 2021; Wang et al., 2021), with <1 indicating simple mono-layer sorption
404 and >6 indicating coprecipitation (Tipping et al., 2002; Wagai and Mayer, 2007). Our
405 findings suggested that the average Fe-OC:Fe_d molar ratio was 10.50 ± 1.91 at the
406 continental scale. However, we could see that the Fe-OC:Fe_d molar ratios (mean 70.18
407 ± 13.82 ; range 2.58–331.68) were much higher in permafrost regions of the Tibetan



408 Plateau than in other specific terrestrial ecosystems, resulting from relatively high Fe-
409 OC and low Fe_d (Mu et al., 2016). In view of the very high molar ratio, coprecipitation
410 is the dominant bonding mechanism of OC and Fe, which contributes to $fFe-OC$
411 reaching 59.5% (average $19.5 \pm 12.3\%$) in Fe-poor (range $0.03\text{--}2.68 \text{ mg g}^{-1}$ soil)
412 permafrost soils of the Tibetan Plateau (Mu et al., 2016). If the permafrost region of the
413 Tibetan Plateau is excluded, the $Fe-OC:Fe_d$ molar ratio in global terrestrial ecosystems
414 was only 3.74 ± 0.47 , indicating that coprecipitation will become a less important
415 bonding mechanism. Recently, a regional-scale survey including typical grasslands,
416 shrublands and forests by Wang et al. (2021) reported that the average $Fe-OC:Fe_d$ molar
417 ratio was 3.0 ± 0.5 (Wang et al., 2021), which lends further credence to the findings
418 mentioned above. The average $Fe-OC:Fe_d$ molar ratio was 2.56 ± 0.19 ($n = 320$; range
419 $0.04\text{--}31.59$) in global marine ecosystems, similar to that of the Bohai Sea (1.59 ± 1.37)
420 (Wang et al., 2019), the Southern Yellow Sea (1.68 ± 1.80) (Ma et al., 2018), East China
421 Sea (1.53 ± 1.28) (Ma et al., 2018), and Barents Sea (2.56 ± 1.76) (Faust et al., 2021),
422 but was much lower than the previous average of global oceans ($n = 42$; 6.10 ± 7.5)
423 (Lalonde et al., 2012), Arctic shelf (Salvadó et al., 2015), and intermediate/old river
424 delta (Shields et al., 2016). Moreover, in wetlands, the molar ratios of $Fe-OC:Fe_d$ were
425 higher (13.47 ± 1.81) than those in continental and marine ecosystems. These results
426 were in accordance with previous findings in regional-scale wetlands (12.78 ± 2.43)
427 (Wang et al., 2021) and coastal wetlands (11.0 ± 4.5) (Bai et al., 2021) but higher than
428 that peatlands (mean 6.53) (Huang et al., 2021). This suggested that the interaction
429 between OC and Fe in wetland ecosystems is mainly dominated by coprecipitation at



430 the global scale, with a molar ratio of >6 usually. Overall, across the global ecosystem
431 types, the average proportion of $\text{Fe-OC}:\text{Fe}_d > 1$ ranged from 60 to 80% (Fig. 5), which
432 indicated the importance of both adsorption and coprecipitation interactions.
433 Furthermore, we found that SOC content could enhance the molar ratio of $\text{Fe-OC}:\text{Fe}_d$
434 by positively regulating Fe-OC content. At the continental scale, climate variables
435 (MAT, MAP) can negatively regulate the molar ratio by changing the Fe_d content (Fig.
436 6a), while in wetlands, soil pH changes the Fe-OC content and then negatively regulates
437 the molar ratio (Fig. 6c). Despite the molar ratio being widely used as an important
438 indicator of the bonding mechanism of Fe and OC, recent studies have shown that only
439 a portion of reactive Fe (25.7–62.6%) was directly associated with OC (Barber et al.,
440 2017). Thus, using the raw $\text{Fe-OC}:\text{Fe}$ molar ratio may result in an underestimation of
441 the actual molar ratio due to the existence of OC-free Fe_d (Wang et al., 2019; Faust et
442 al., 2021). At neutral to alkaline pH, associated with arid and semiarid soils, the
443 association of reactive Fe and OC is limited (Sowers et al., 2018a; Sowers et al., 2018b),
444 while calcium (Ca) is especially important in OC binding via Ca bridging (Sowers et
445 al., 2018a; Wang et al., 2021). Wang et al. (2021) provided direct evidence that the Fe-
446 OC determined by the classic BCD method contained Ca-bound OC, accounting for
447 approximately 24% of Fe-OC (Wang et al., 2021), and the $\text{Fe-OC}:\text{Fe}_d$ molar ratio might,
448 therefore, be overestimated, for example, in the permafrost regions of the Tibetan
449 Plateau (soil pH 8.01–9.52) (Mu et al., 2016). Therefore, to draw a valid inference on
450 the bonding mechanisms of OC and reactive Fe, further work is necessary to unravel
451 the complex mechanisms.



452 5. Conclusions

453 To our knowledge, this is the first study to reveal the patterns and drivers of Fe-
454 OC across global ecosystems (Fig. 7). More importantly, our global-scale results
455 showed that Fe-OC was an important fraction of SOC at the continental scale, in
456 wetlands, and in marine ecosystems. Our findings highlighted that some drivers for Fe-
457 OC associations are valid globally, but those ecosystem-specific predictors should also
458 be uncovered. Correlation analysis and RF modelling indicated that the Fe-OC:Fe_d
459 molar ratio and SOC were the predominant predictors of Fe-OC and *f*Fe-OC compared
460 with climate variables and soil pH in global ecosystems. The Fe-OC:Fe_d molar ratio
461 was the predominant driver of Fe-OC at the continental scale and in wetlands, whereas
462 Fe_d content was a good predictor in the global marine ecosystem, improving our ability
463 to predict Fe-OC variations among ecosystem types. Moreover, in global wetlands, the
464 fractions of Fe-OC in total SOC may be increasing in response to climate warming. As
465 an indicator of the Fe and OC bonding mechanism, the molar ratio between 1–6 (<1 for
466 adsorption, >6 for coprecipitation) in global ecosystems exceeds 60%, highlighting the
467 importance of the interactions of both adsorption and coprecipitation. Compared with
468 continental and marine ecosystems, coprecipitation plays a more important role in
469 wetlands due to the high molar ratio. Our findings provide direct evidence that reactive
470 Fe minerals are a dominant natural mechanism for long-term SOC storage in global
471 ecosystems.



472 **Acknowledgments**

473 We are very grateful to all the researchers whose data were compiled in this study. This
474 study was supported by the National Natural Science Foundation of China (32101333).

475 **Conflict of interest**

476 The authors declare that they have no known competing financial interests or personal
477 relationships that could have appeared to influence the work reported in this paper.

478 **Data availability statement**

479 The data that supports the findings of this study are available in the Supporting Data
480 Set.

481



482 **References**

- 483 Adhikari, D., Poulson, S. R., Sumaila, S., Dynes, J. J., McBeth, J. M., and Yang, Y.: Asynchronous
484 reductive release of iron and organic carbon from hematite–humic acid complexes, *Chem.*
485 *Geol.*, 430, 13-20, <https://doi.org/10.1016/j.chemgeo.2016.03.013>, 2016
- 486 Anthony, T. L., and Silver, W. L.: Mineralogical associations with soil carbon in managed wetland
487 soils, *Global Change Biol.*, 26, 6555-6567, <https://doi.org/10.1111/gcb.15309>, 2020.
- 488 Bai, J., Luo, M., Yang, Y., Xiao, S., Zhai, Z., and Huang, J.: Iron-bound carbon increases along a
489 freshwater-oligohaline gradient in a subtropical tidal wetland, *Soil Biol. Biochem.*, 154,
490 108128, <https://doi.org/10.1016/j.soilbio.2020.108128>, 2021.
- 491 Barber, A., Brandes, J., Leri, A., Lalonde, K., Balind, K., Wirick, S., Wang, J., and Gelinis, Y.:
492 Preservation of organic matter in marine sediments by inner-sphere interactions with reactive
493 iron, *Sci. Rep.*, 7, 366, <https://doi.org/10.1038/s41598-017-00494-0>, 2017.
- 494 Berner, R. A.: Sedimentary pyrite formation, *Am. J. Sci.*, 268, 1-23. [https://doi.org/10.2475/](https://doi.org/10.2475/ajs.268.1.1)
495 [ajs.268.1.1](https://doi.org/10.2475/ajs.268.1.1), 1970.
- 496 Bhattacharyya, A., Campbell, A. N., Tfaily, M. M., Lin, Y., Kukkadapu, R. K., Silver, W. L., Nico,
497 P. S., and Pett-Ridge, J.: Redox fluctuations control the coupled cycling of iron and carbon in
498 tropical forest soils, *Environ. Sci. Technol.*, 52, 14129-14139, [https://doi.org/10.1021/](https://doi.org/10.1021/acs.est.8b03408)
499 [acs.est.8b03408](https://doi.org/10.1021/acs.est.8b03408), 2018.
- 500 Bridgman, S. D., Megonigal, J. P., Keller, J. K., Bliss, N. B., and Trettin, C.: The carbon balance of
501 North American wetlands, *Wetlands*, 26, 889-916, <https://doi.org/10.1023/A:1010933404324>,
502 2006.
- 503 Carter, A. J., and Scholes, R. J.: Spatial global database of soil properties. In: IGBP Global Soil Data
504 Task (Database on CD-ROM), International Geosphere-Biosphere Programme (IGBP) Data
505 Information Systems, producer. Toulouse: IGBP, 2000.
- 506 Chen, C., Dynes, J. J., Wang, J., and Sparks, D. L.: Properties of Fe-organic matter associations via
507 coprecipitation versus adsorption, *Environ. Sci. Technol.*, 48, 13751-13759, [https://doi.org/](https://doi.org/10.1021/es503669u)
508 [10.1021/es503669u](https://doi.org/10.1021/es503669u), 2014.
- 509 Chien, S.C., and Krumins, J. A.: Natural versus urban global soil organic carbon stocks: A meta-
510 analysis, *Sci. Total Environ.*, 807, 150999, <https://doi.org/10.1016/j.scitotenv.2021.150999>,



- 511 2022.
- 512 Cotrufo, M. F., Ranalli, M. G., Haddix, M. L., Six, J., and Lugato, E.: Soil carbon storage informed
513 by particulate and mineral-associated organic matter, *Nat. Geosci.*, 12, 989-994,
514 <https://doi.org/10.1038/s41561-019-0484-6>,2019.
- 515 Coward, E. K., Thompson, A., Plante, A. F.: Contrasting Fe speciation in two humid forest soils:
516 Insight into organomineral associations in redox-active environments, *Geochim. Cosmochim.*
517 *Ac.*, 238, 68-84, <https://doi.org/10.1016/j.gca.2018.07.007>,2018.
- 518 Crowther, T. W., Todd-Brown, K. E., Rowe, C. W., et al.: Quantifying global soil carbon losses in
519 response to warming, *Nature*, 540, 104-108, <https://doi.org/10.1038/nature20150>,2016.
- 520 Delgado-Baquerizo, M., Grinyer, J., Reich, P. B., and Singh, B. K.: Relative importance of soil
521 properties and microbial community for soil functionality: insights from a microbial swap
522 experiment, *Funct. Ecol.*, 30, 1862-1873, <https://doi.org/10.1111/1365-2435.12674>,2016.
- 523 Eusterhues, K., Rumpel, C., Kogel-Knabner, I.: Organo-mineral associations in sandy acid forest
524 soils: importance of specific surface area, iron oxides and micropores, *Eur. J. Soil Sci.*, 56, 753-
525 763, <https://doi.org/10.1111/j.1365-2389.2005.00710.x>, 2005.
- 526 Fang, K., Qin, S., Chen, L., Zhang, Q., Yang, Y.: Al/Fe mineral controls on soil organic carbon stock
527 across tibetan alpine grasslands, *J. Geophys. Res-Bioge.*, 124, 247-259, <https://doi.org/10.1029/2018JG004782>,2019.
- 529 Faust, J. C., Tessin, A., Fisher, B. J., Zindorf, M., Papadaki, S., Hendry, K. R., Doyle, K. A., and
530 März, C.: Millennial scale persistence of organic carbon bound to iron in Arctic marine
531 sediments, *Nat. Commun.*, 12, 275, <https://doi.org/10.1038/s41467-020-20550-0>,2021.
- 532 Fisher, B. J., Moore, O. W., Faust, J. C., Peacock, C. L., and März, C.: Experimental evaluation of
533 the extractability of iron bound organic carbon in sediments as a function of carboxyl content,
534 *Chem. Geol.*, 556, 119853, <https://doi.org/10.1016/j.chemgeo.2020.119853>,2020.
- 535 Freeman, C., Ostle, N., and Kang, H.: An enzymic 'latch' on a global carbon store, *Nature*, 409, 149-
536 149, <https://doi.org/10.1038/35051650>,2001.
- 537 Grybos, M., Davranche, M., Gruau, G., Petitjean, P., and Pédrot, M.: Increasing pH drives organic
538 matter solubilization from wetland soils under reducing conditions, *Geoderma*, 154, 13-19,
539 <https://doi.org/10.1016/j.geoderma.2009.09.001>,2009.



- 540 Guggenberger, G., and Kaiser, K.: Dissolved organic matter in soil: challenging the paradigm of
541 sorptive preservation, *Geoderma*, 113, 293-310, [https://doi.org/10.1016/S0016-](https://doi.org/10.1016/S0016-7061(02)00366-X)
542 7061(02)00366-X,2003.
- 543 Hemingway, J. D., Rothman, D. H., Grant, K. E., Rosengard, S. Z., Eglinton, T. I., Derry, L. A., and
544 Galy, V. V.: Mineral protection regulates long-term global preservation of natural organic
545 carbon, *Nature*, 570, 228-231, <https://doi.org/10.1038/s41586-019-1280-6>,2019.
- 546 Hopkinson, C. S., Cai, W. J., and Hu, X.: Carbon sequestration in wetland dominated coastal
547 systems—a global sink of rapidly diminishing magnitude, *Curr. Opin. Env. Sust.*, 4, 186-194,
548 <https://doi.org/10.1016/j.cosust.2012.03.005>,2012.
- 549 Huang, W., and Hall, S. J.: Elevated moisture stimulates carbon loss from mineral soils by releasing
550 protected organic matter, *Nat. Commun.*, 8, 1-10, [https://doi.org/10.1038/s41467-017-01998-](https://doi.org/10.1038/s41467-017-01998-z)
551 z,2017.
- 552 Huang, X., Liu, X., Liu, J., Chen, H.: Iron-bound organic carbon and their determinants in peatlands
553 of China, *Geoderma*, 391, <https://doi.org/10.1016/j.geoderma.2021.114974>,2021.
- 554 Jones, A.M., Griffin, P.J., Waite, T.D.: Ferrous iron oxidation by molecular oxygen under acidic
555 conditions: The effect of citrate, EDTA and fulvic acid, *Geochim. Cosmochim. Ac.*, 160, 117-
556 131, <https://doi.org/10.1016/j.gca.2015.03.026>, 2015.
- 557 Kaiser, K., and Guggenberger, G.: Mineral surfaces and soil organic matter, *Eur. J. Soil Sci.*, 54,
558 219-236, <https://doi.org/10.1046/j.1365-2389.2003.00544.x>,2003.
- 559 Kaiser, K., Mikutta, R., and Guggenberger, G.: Increased stability of organic matter sorbed to
560 ferrihydrite and goethite on aging, *Soil Sci. Soc. Am. J.*, 71, 711-719, [https://doi.org/10.2136/](https://doi.org/10.2136/sssaj2006.0189)
561 /sssaj2006.0189,2007.
- 562 Kramer, M.G., and Chadwick, O.A.: Climate-driven thresholds in reactive mineral retention of soil
563 carbon at the global scale, *Nat. Clim. Change*, 8, 1104-1108, [https://doi.org/10.1038/s41558-](https://doi.org/10.1038/s41558-018-0341-4)
564 018-0341-4,2018.
- 565 LaCroix, R.E., Tfaily, M.M., McCreight, M., Jones, M.E., Spokas, L., and Keiluweit, M.: Shifting
566 mineral and redox controls on carbon cycling in seasonally flooded mineral soils,
567 *Biogeosciences*, 16, 2573-2589, <https://doi.org/10.5194/bg-16-2573-2019>,2019.
- 568 Lal, R.: Soil carbon sequestration impacts on global climate change and food security, *Science*, 304,



- 569 1623-1627, <https://doi.org/10.1126/science.1097396>,2004a.
- 570 Lal, R.: Soil carbon sequestration to mitigate climate change, *Geoderma*, 123, 1-22,
571 <https://doi.org/10.1016/j.geoderma.2004.01.032>,2004b.
- 572 Lalonde, K., Mucci, A., Ouellet, A., and Gelinas, Y.: Preservation of organic matter in sediments
573 promoted by iron, *Nature*, 483, 198-200, <https://doi.org/10.1038/nature10855>,2012.
- 574 Longman, J., Faust, J.C., Bryce, C., Homoky, W.B., März, C.: Organic carbon burial with reactive
575 iron across global environments, *Global Biogeochem. Cy.* 36, <https://doi.org/10.1029/2022gb007447>,2022.
- 577 Ma, W. W., Zhu, M. X., Yang, G. P., and Li, T.: Iron geochemistry and organic carbon preservation
578 by iron (oxyhydr) oxides in surface sediments of the East China Sea and the south Yellow Sea,
579 *J. Marine Syst.*, 178, 62-74, <https://doi.org/10.1016/j.jmarsys.2017.10.009>,2018.
- 580 McLeod, E., Chmura, G. L., Bouillon, S., Salm, R., Björk, M., Duarte, C. M., Lovelock, C. E.,
581 Schlesinger, W. H., and Silliman, B. R.: A blueprint for blue carbon: toward an improved
582 understanding of the role of vegetated coastal habitats in sequestering CO₂, *Front. Ecol.*
583 *Environ.*, 9, 552-560, <https://doi.org/10.1890/110004>,2011.
- 584 Meisner, A., Gera Hol, W. H., de Boer, W., Krumins, J. A., Wardle, D. A., and van der Putten, W.H.:
585 Plant–soil feedbacks of exotic plant species across life forms: a meta-analysis, *Biol. Invasions*,
586 16, 2551-2561, <https://doi.org/10.1007/s10530-014-0685-2>,2014.
- 587 Mu, C. C., Zhang, T. J., Zhao, Q., Guo, H., Zhong, W., Su, H., and Wu, Q. B.: Soil organic carbon
588 stabilization by iron in permafrost regions of the Qinghai-Tibet Plateau, *Geophys. Res. Lett.*,
589 43, 10, 286-294, <https://doi.org/10.1002/2016GL070071>,2016.
- 590 Pan, Y. D., Birdsey, R. A., Fang, J. Y., Houghton, R., Kauppi, P. E., Kurz, W. A., et al.: A large and
591 persistent carbon sink in the world's forests, *Science*, 333, 988-993. <https://doi.org/10.1126/science.120160>,2011.
- 593 Patzner, M. S., Mueller, C. W., Malusova, M., Baur, M., Nikeleit, V., Scholten, T., Hoeschen, C.,
594 Byrne, J.M., Borch, T., and Kappler, A.: Iron mineral dissolution releases iron and associated
595 organic carbon during permafrost thaw, *Nat. Commun.*, 11, 1-11, <https://doi.org/10.1038/s41467-020-20102-6>,2020.
- 597 Peter, S., and Sobek, S.: High variability in iron-bound organic carbon among five boreal lake



- 598 sediments, *Biogeochemistry*, 139, 19-29, <https://doi.org/10.1007/s10533-018-0456-8>, 2018.
- 599 Riedel, T., Zak, D., Biester, H., Dittmar, T.: Iron traps terrestrially derived dissolved organic matter
600 at redox interfaces. *Proc. Natl. Acad. Sci. USA.*, 110, 10101-10105, [https://doi.org/](https://doi.org/10.1073/pnas.1221487110)
601 [10.1073/pnas.1221487110](https://doi.org/10.1073/pnas.1221487110), 2013.
- 602 Roulet, N. T.: Peatlands, carbon storage, greenhouse gases, and the Kyoto Protocol: Prospects and
603 significance for Canada, *Wetlands*, 20, 605-615, [https://doi.org/10.1672/0277-5212\(2000\)020](https://doi.org/10.1672/0277-5212(2000)020)
604 [\[0605:PCSGGA\]2.0.CO;2](https://doi.org/10.1672/0277-5212(2000)020), 2000.
- 605 Salvadó, J. A., Tesi, T., Andersson, A., Ingri, J., Dudarev, O. V., Semiletov, I. P., Gustafsson, Ö.:
606 Organic carbon remobilized from thawing permafrost is resequenced by reactive iron on the
607 Eurasian Arctic Shelf, *Geophys. Res. Lett.*, 42, 8122-8130, <https://doi.org/10.1002/2015>
608 [GL066058](https://doi.org/10.1002/2015), 2015.
- 609 Schmidt, M. W., Torn, M.S., Abiven, S., Dittmar, T., Guggenberger, G., Janssens, I.A., Kleber, M.,
610 Kogel-Knabner, I., Lehmann, J., Manning, D. A., Nannipieri, P., Rasse, D. P., Weiner, S., and
611 Trumbore, S. E.: Persistence of soil organic matter as an ecosystem property, *Nature*, 478, 49-
612 56, <https://doi.org/10.1038/nature10386>, 2011.
- 613 Shields, M. R., Bianchi, T. S., Gélinas, Y., Allison, M. A., and Twilley, R. R.: Enhanced terrestrial
614 carbon preservation promoted by reactive iron in deltaic sediments, *Geophys. Res. Lett.*, 43,
615 1149-1157. <https://doi.org/10.1002/2015GL067388>, 2016.
- 616 Smale, D.A., Wernberg, T., Oliver, E.C.J., Thomsen, M., Harvey, B.P., and Straub, S.C., et al.:
617 Marine heatwaves threaten global biodiversity and the provision of ecosystem services, *Nat.*
618 *Clim. Change*, 9, 306-312. <https://doi.org/10.1038/s41558-019-0412-1>, 2019.
- 619 Sowers, T. D., Adhikari, D., Wang, J., Yang, Y., and Sparks, D. L.: Spatial associations and chemical
620 composition of organic carbon sequestered in Fe, Ca, and organic carbon ternary systems,
621 *Environ. Sci. Technol.*, 52, 6936-6944, <https://doi.org/10.1021/acs.est.8b01158>, 2018a.
- 622 Sowers, T. D., Stuckey, J. W., and Sparks, D. L.: The synergistic effect of calcium on organic carbon
623 sequestration to ferrihydrite, *Geochem. T.*, 19, 4 [https://doi.org/10.1186/s12932-018-0049-](https://doi.org/10.1186/s12932-018-0049-4)
624 [4](https://doi.org/10.1186/s12932-018-0049-4), 2018b.
- 625 Tipping, E., Rey-Castro, C., Bryan, S. E., and Hamilton-Taylor, J.: Al(III) and Fe(III) binding by
626 humic substances in freshwaters, and implications for trace metal speciation, *Geochim.*



- 627 Cosmochim. Ac., 66, 3211-3224, [https://doi.org/10.1016/S0016-7037\(02\)00930-4](https://doi.org/10.1016/S0016-7037(02)00930-4),2002.
- 628 Wagai, R., and Mayer, L. M.: Sorptive stabilization of organic matter in soils by hydrous iron oxides,
629 Geochim. Cosmochim. Ac., 71, 25-35, <https://doi.org/10.1016/j.gca.2006.08.047>,2007.
- 630 Wan, D., Ye, T. H., Lu, Y., Chen, W. L., Cai, P., Huang, Q. Y.: Iron oxides selectively stabilize plant-
631 derived polysaccharides and aliphatic compounds in agricultural soils, Eur. J. Soil Sci., 70,
632 1153-1163, <https://doi.org/10.1111/ejss.12827>,2019.
- 633 Wang, D., Zhu, M. X., Yang, G. P., and Ma, W. W.: Reactive iron and iron-bound organic carbon in
634 surface sediments of the river-dominated Bohai Sea (China) versus the Southern Yellow Sea.
635 J. Geophys. Res-Biogeo., 124, 79-98, <https://doi.org/10.1029/2018JG004722>,2019.
- 636 Wang, S., Jia, Y., Liu, T., Wang, Y., Liu, Z., and Feng, X.: Delineating the role of calcium in the
637 large-scale distribution of metal-bound organic carbon in soils, Geophys. Res. Lett., 48,
638 e2021GL092391, <https://doi.org/10.1029/2021GL092391>,2021.
- 639 Wang, Y., Wang, H., He, J.S., and Feng, X.: Iron-mediated soil carbon response to water-table
640 decline in an alpine wetland, Nat. Commun., 8, 1-9, <https://doi.org/10.1038/ncomms15972>,
641 2017.
- 642 Ye, C., Huang, W., Hall, S.J., and Hu, S.: Association of organic carbon with reactive iron oxides
643 driven by soil pH at the global scale, Global Biogeochem. Cy., 36, e2021GB007128,
644 <https://doi.org/10.1029/2021GB007128>,2022.
- 645 Yu, C., Xie, S., Song, Z., Xia, S., and Åström, M. E.: Biogeochemical cycling of iron (hydr-) oxides
646 and its impact on organic carbon turnover in coastal wetlands: A global synthesis and
647 perspective, Earth-Sci. Rev., 218, 103658, <https://doi.org/10.1016/j.earscirev.2021.103658>,
648 2021.
- 649 Zhao, B., Jia, Y., Wu, S., Wei, L., Li, J., Hong, H., Yan, C., Williams, M.A., and Wang, Q.:
650 Preservation of soil organic carbon in coastal wetlands promoted by glomalin–iron–organic
651 carbon ternary system, Limnol. Oceanogr., 67, S180-S192, <https://doi.org/10.1002/lno.12238>,2022.
- 652 Zhao, Q., Poulson, S. R., Obrist, D., Sumaila, S., Dynes, J. J., McBeth, J. M., Yang, Y.: Iron-bound
653 organic carbon in forest soils: quantification and characterization, Biogeosciences, 13, 4777-
654 4788, <https://doi.org/10.5194/bg-13-4777-2016>, 2016.
- 655 Zong, M., Lin, C., Li, S., Li, H., Duan, C., Peng, C., Guo, Y. M., and An, R.: Tillage activates iron



656 to prevent soil organic carbon loss following forest conversion to cornfields in tropical acidic
657 red soils, *Sci. Total Environ.*, 761, 143253. <https://doi.org/10.1016/j.scitotenv.2020.143253>,
658 2021.

659 **Figure captions**

660 **Fig. 1** Global distribution of study sites.

661 **Fig. 2** The Fe-OC content (a), *f*Fe-OC (b), soil pH (c), Fe_d content (d), SOC content (e),
662 and Fe-OC/Fe_d molar ratio (f) in different ecosystems shown in the box-plot. Solid dots
663 indicate outliers, and imaginary points represent observations. Box edges are upper and
664 lower quartiles; central lines are median value; whiskers represent standard error. The
665 differences among continental, wetland and marine ecosystems are illustrated (* $p <$
666 0.05, ** $p < 0.01$, *** $p < 0.001$).

667 **Fig. 3** Relationships between Fe-OC, *f*Fe-OC and soil properties (soil pH, Fe_d, Fe-
668 OC/Fe_d molar ratio, SOC, clay), climate variables (MAT, MAP) and latitude across
669 global ecosystem types. The line represents the line of best fit for each ecosystem, and
670 the shaded area indicates the 95% confidence interval for the global dataset. In marine
671 ecosystems, the climate variables (MAT, MAP) and soil pH are not shown due to limited
672 data.

673 **Fig. 4** The relative importance of climate variables (MAT, MAP), soil properties (SOC,
674 soil pH, Fe-OC:Fe_d, and Fe_d), and geographical location (i.e., latitude) for Fe-OC and
675 *f*Fe-OC in continents (a, b), marine ecosystems (c, d), and wetlands (e, f) by random
676 forest (RF) analysis. The mean square error (MSE) is used to estimate the importance



677 of these predictors, with higher MSE values indicating more important predictors. In
678 marine ecosystems, the climate variables (MAT, MAP) and soil pH are not shown due
679 to limited data. Ratio: Fe-OC/Fe_d molar ratio. Asterisks show significant differences:
680 * $p < 0.05$, and ** $p < 0.01$.

681 **Fig. 5** Frequency distributions of the Fe-OC/Fe_d molar ratio in different ecosystems.
682 The molar ratio of Fe-OC:Fe_d is used as an indicator of Fe/OC interaction types, which
683 is < 1.0 for adsorption and > 6 for coprecipitation (Wagai and Mayer, 2007; Wang et al.,
684 2017).

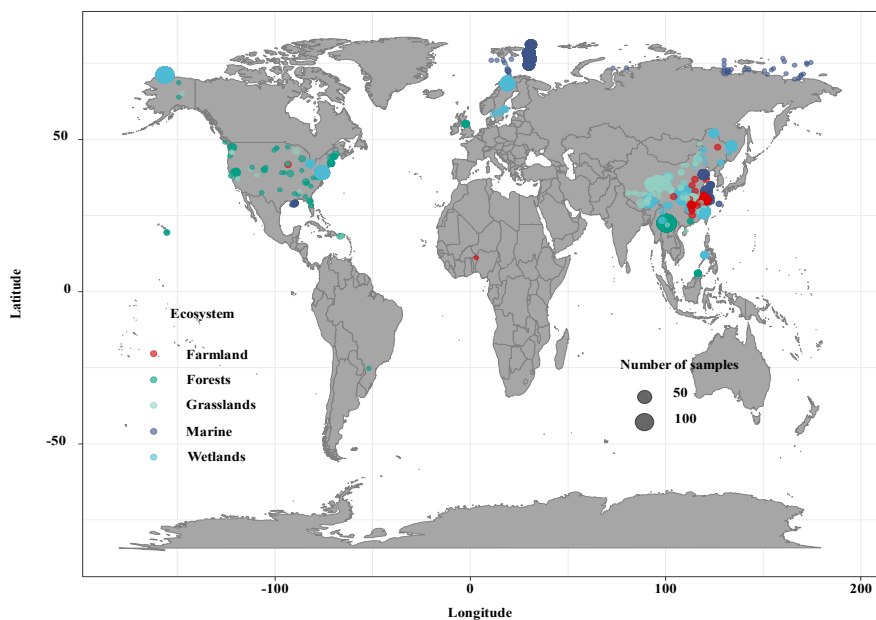
685 **Fig. 6** The Spearman correlation analysis results of the Fe-OC, Fe-OC/Fe_d molar ratio
686 (i.e., ratio) and environmental factors (MAT, MAP, pH) in continental (a), marine (b)
687 and wetland ecosystems (c). Asterisks show significant differences: * $p < 0.05$, ** $p <$
688 0.01 , and *** $p < 0.001$.

689 **Fig. 7** Schematic representation of drivers, dynamic and patterns of Fe-OC associations
690 in different ecosystem types on global scale. Data are averages of different ecosystem
691 types. A lower SOC molecular diversity and concomitant lower contents of Fe-OC (e.g.,
692 sea and continent ecosystems), whereas higher diversity increases the Fe-OC contents
693 (e.g., wetlands). However, there was no significant difference in the proportion of Fe-
694 OC in total SOC. The asterisk (*) indicates significant differences.

695



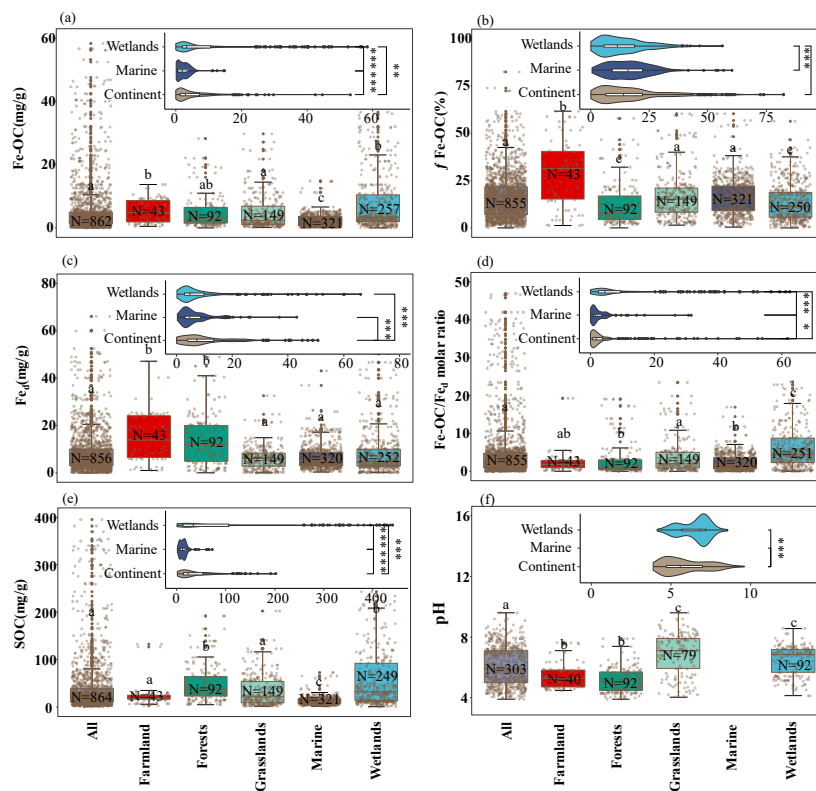
696 **Figure 1**



697



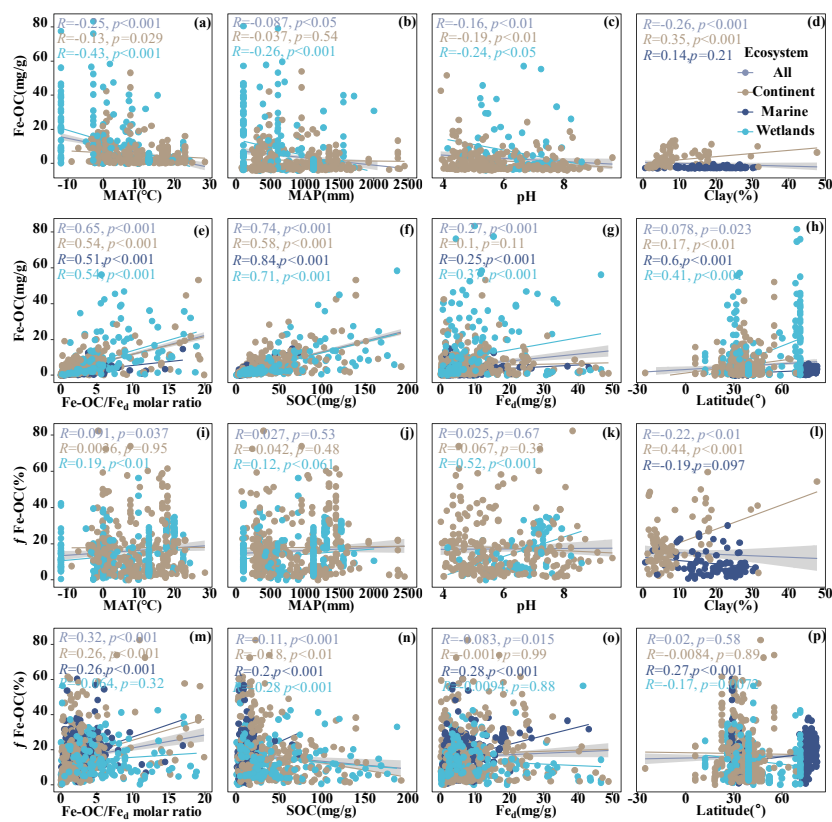
698 **Figure 2**



699



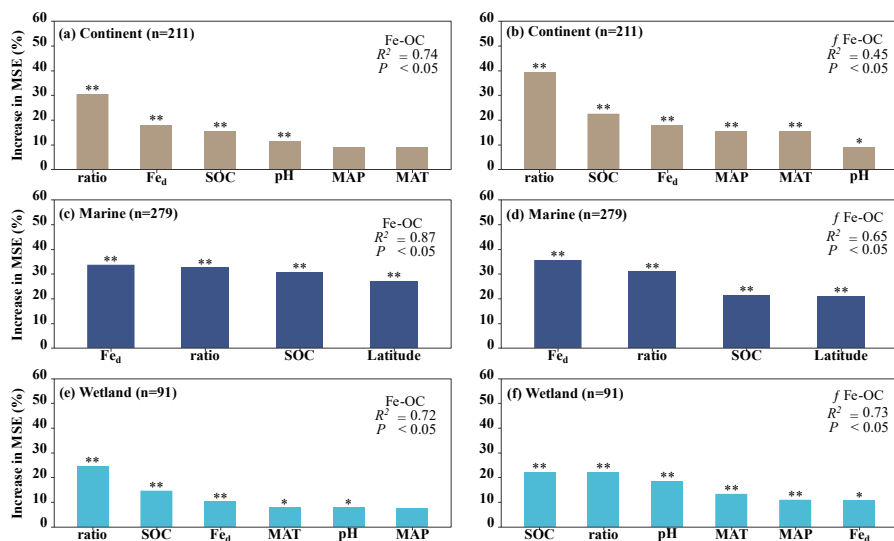
700 **Figure 3**



701



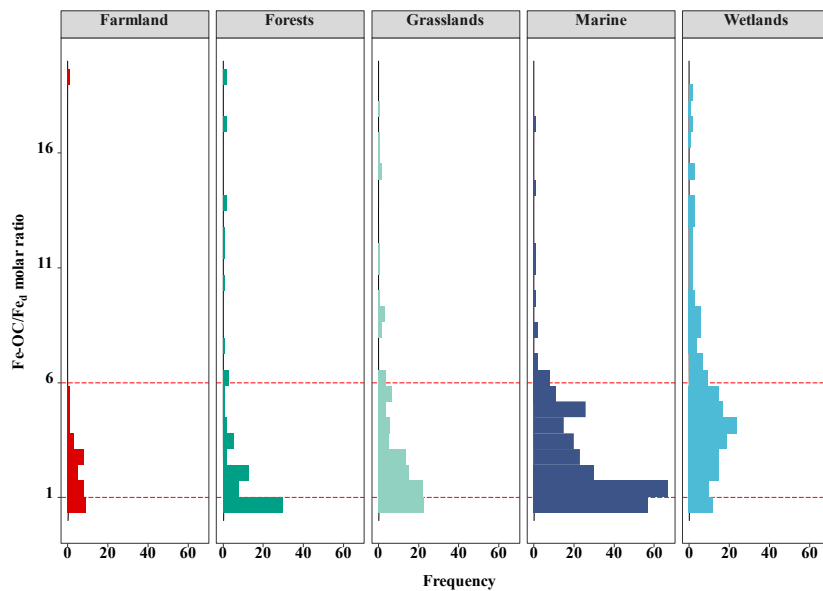
702 **Figure 4**



703



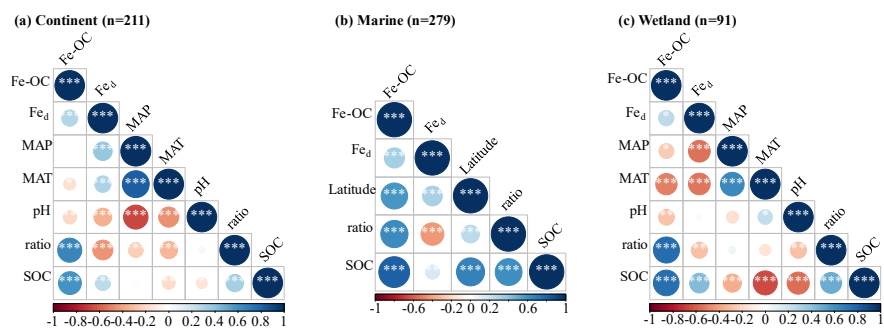
704 **Figure 5**



705



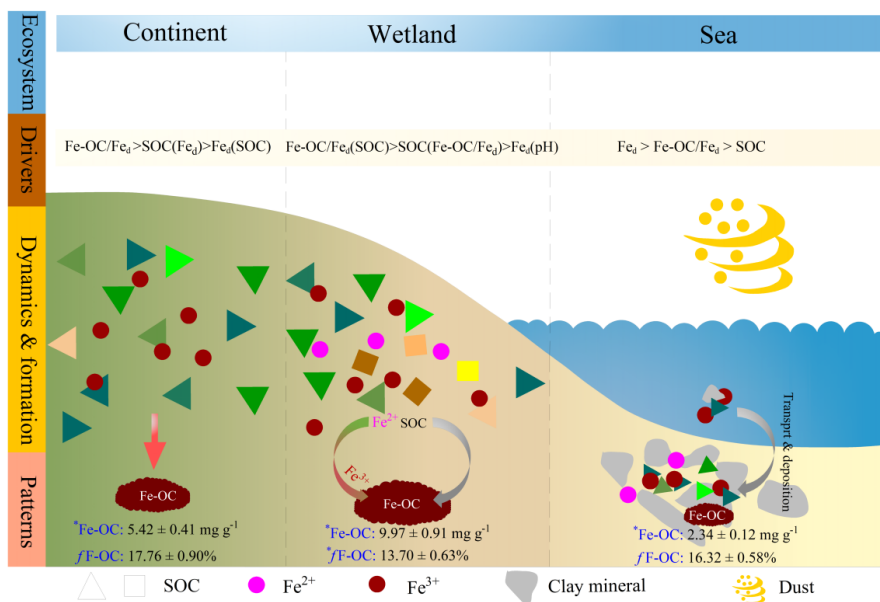
706 **Figure 6**



707



708 **Figure 7**



709